Simulation algorithm of sample strategy for CMM based on Neural Network Approach

Petr Chelishchev[1] and Knut Sørby[1]

[1] Department of Mechanical and Industrial Engineering, NTNU, NO-7491 Trondheim, Norway

petr.chelishchev@ntnu.no

Abstract. This paper proposes the algorithm for analyses of sample strategies. The back propagation artificial neural network approach is employed to approximate CMM measurements of the circular features of the aluminum workpieces machined with milling process. The discrete data is transformed into continuous nondeterministic profiles. The profiles are used for simulation to estimate the maximum possible error in different sample strategies for various diameters.

Keywords: Neural network, deep learning, nondeterministic profile, sample strategy, CMM.

1 Introduction

Coordinate Measuring Machines (CMMs) play an important role in the part inspection and quality control [1]. One of the important parameters in measuring strategy with CMM is the sample size of measuring points. The sample-point measurements provide discrete coordinates of the workpiece surface. The point-coordinates are used for assessment whether a form or dimension deviation are inside or outside of tolerance limits. The optimal choice of discrete points also relatives with applied evaluation methods and tolerance types [2], [3]. The reliability and quality of CMM sample assessment depends on density and location of measured points [4]. Thus, the inspection is often a compromise between a required time, cost, and the measuring uncertainty.

The result of measuring inspection depends on manufacturing process errors as well. Mesay et al. [5] have classified the process error into systematic and random components. In another paper, Qimi, Mesay et al. [6] have estimated the frequency of systematic errors by use of Fourier analyses. Other authors have investigated the measuring uncertainty due to the sample size based on approximation of aperiodic deterministic profile with Fourier series [7], [8].

Moschos et. al [9] suggested a Bayesian regularized artificial neural network (BRANN) model trained with relatively small sample size to predict a variability of large data sample. Other authors determine an optimal inspection sample size based on measuring errors approximated by ANN for various machine processes and nominal sizes [10].

A workpiece profile cannot be prescribed before it is measured, thus the profile is characterized as nondeterministic. This paper deals with the nondeterministic profiles derived from coordinate measurements of real workpieces. In order to investigate an influence of the sample size, Artificial Neural Network (ANN) was employed to create the continues nondeterministic profiles based on the discrete CMM data.

2 Artificial Neural Network approach

The state of the art in Artificial Neural Network is based on our understanding level of biological neurons function [11]. One of the most important advantage of ANN is that it can mimic processes with unknown relation of input and output data. In the case of limited information about a complex process, the ANN can provide relatively precise solution based on limited experimental data. The artificial network composed of differently connected artificial neurons, which are named as processing elements (PE). The PEs are connected into input layers, hidden layers, and output layers to create the artificial network [12]. Multilayers ANN can include many layers but to reduce the computation time, most commercial systems do not exceed two layers. It is important to notice that the final solution of ANN is not unique, but the one that satisfies the minimal error requirements.

A multiple feed forward back-propagation (PB) ANN [13], was created in MATLAB program environment (Fig. 1). The design of PB ANN includes a number of steps [14] such as: preparing and pre-processing of training data; creating of a network structure; configuring the network; initialization weights and biases; training, validation and testing of the network.Let us have a look at each of these steps in detail.

We denote φ_k as the network input and R_k as the target, thus we have a network with one input and one output. In order to achieve a better accuracy we apply a deep leaning strategy in this work. There are two hidden layers, with 260 neurons in the first and 12 neurons in the second layer. The chosen number of layers, neurons is a trial and error procedure.

In our case, we utilize the tan-sigmoid transfer function (*tansig*) for both hidden layers. The *tansig* function has a following form:

$$y = f(a) = \frac{2}{1+e^{-2a}} - 1 \ , \qquad (1)$$

where the argument a is a summation of weights w_{ij} and biases s_i (threshold value) and given by such expression:

$$a = \sum_{i=1}^{n} w_{ij}\varphi_j - s_i \ , \qquad (2)$$

where φ_j is the input.

The linear transfer function (*purelin*) was used for the output layer. The activation functions are defined over the interval [-1, 1].

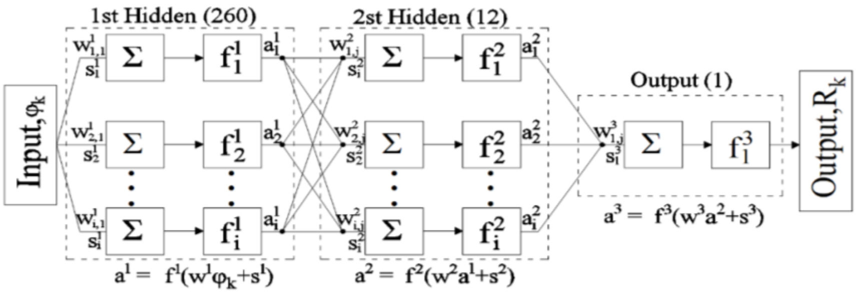

Fig. 1. A 1-260-12-1 feed forward ANN architecture for approximation of the measuring profiles

The Levenberg-Marquardt training algorithm was performed for ANN learning [15]. In spite of the fact that this method has larger memory requirements than other approaches, it is the fastest supervised optimization algorithm with an efficient implementation in MATLAB. The algorithm regulates whether the Newton or the Gradient Decent method is performed. In such case we must use the mean squared error (MSE) obtained as following:

$$MSE = \sum_{i=1}^{m} \frac{(y_i - t_i)^2}{m} , \tag{3}$$

where m is a total set of all entries.

The measurement data was divided as the following: training – 85 % ; validation – 10 %; test – 5 %. The procedure described above was repeated until maximum absolute error $|\varepsilon_{\max}|$ reaches a value below a certain value. In this work $|\varepsilon_{\max}| < 2$ μm was applied.

3 Model Implementation

For implementation of our approach, we measured circular holes milled in a 20 mm aluminium plate. There are 9 holes of various diameters from 40 mm to 500 mm. The inspection was performed in a Leitz PMM-C-600 coordinate measuring machine with an analogue probe and *PC-DMIS* software. The middle section of each hole was measured with 480 uniformly distributed points. The least squares circle (LSC) method was used to calculate the circle centre coordinates (X_c, Y_c) and radius values of each section. Usually, the LSC method overestimates the roundness value compared to the minimum zone (MZ, Chebyshev) method, which is recommended method by ISO 1101 standard. However, in the case of small sample sizes, the true value might be underestimated. Thus, the LSC may be more preferable. Besides, the LSC method is set as default in all previous versions of *PC-DMIS*.

The radius distance R_k from the circle centre (X_c, Y_c) to each individual measured point (X_k, Y_k) was calculated as following:

$$R_k = \sqrt{(X_k - X_c)^2 + (Y_k - Y_c)^2}\ , \qquad (4)$$

The value of the radial angle was set as $\varphi_k = 2\pi \cdot k / 480, k = 0...479$, where k is the index number of measured points. The few examples of such estimated radius variable versus the angle are shown on the polar plots in Fig. 2.

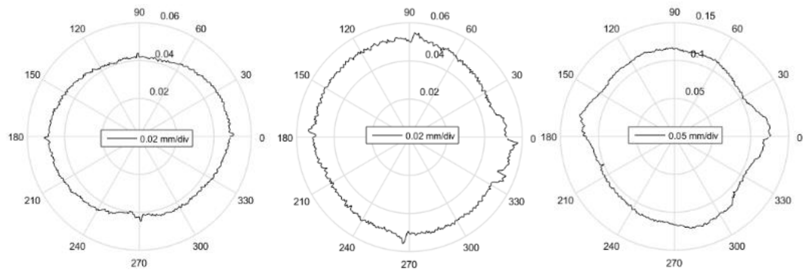

(a) $D_1 = 40$ mm (b) $D_3 = 100$ mm (c) $D_9 = 500$ mm

Fig. 2. The measured profiles of three radial sections

These estimated profiles were approximated with ANN model. An example of the approximated nondeterministic profile is illustrated in Fig. 3. The lowest graph of figure 3 shows the approximations error in each particular point. The total range of the fit errors is within $\pm 0.9 \cdot 10^{-4}$ mm for this particular profile. The nondeterministic profile equivalents to a continuous function, that provides an opportunity to simulate the measuring strategies based on real measurements and perfect repeatability conditions.

4 Simulation procedure

In order to estimate the maximum measuring error due to the sample size, an additional procedure was developed. A common practice in CMM measuring is using the sample consisting of equally distributed measuring points and the LSC as the default method. An example of the simulation, using a five-point sample (n = 5), is illustrated in Fig. 4. A sample of n equally distributed points is taken from the ANN profile (section 2.2), and the n-point sample is rotated clockwise with $m = 10^3$ iteration number. In each iteration the sample is rotated by the angular step $s = 2\pi / nm$. When the first point p_1 position is defined, the other $(n-1)$ sample points ($p_2, p_3, ... p_n$) are determined uniquely with equal space $2\pi / n$. The sample of n radius values r_k^{ANN} ($k = 1,...n$) is generated from the trained network corresponding to uniform point locations.

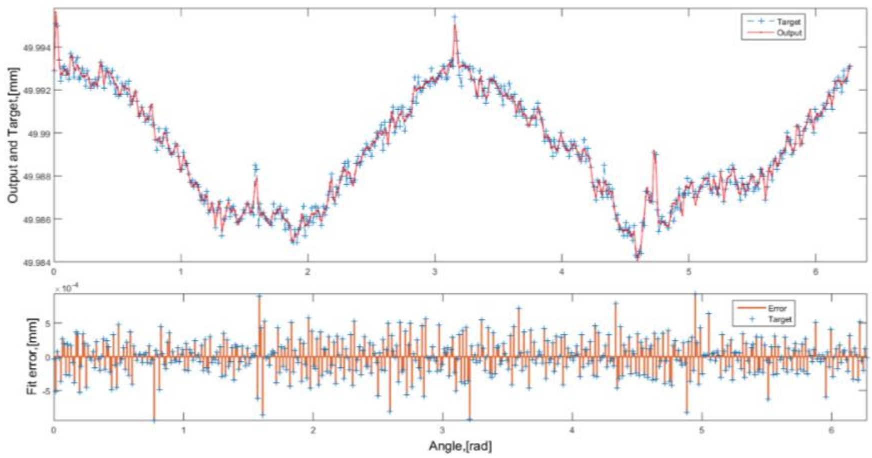

Fig. 3. The continues nondeterministic profile approximated with ANN ($D_3 = 100$ mm)

The corresponding x_k, y_k coordinates are calculated from radius variables r_k^{ANN} by following equations:

$$\begin{cases} x_k = X_c + r_k^{ANN} \cos(\varphi_k) & (5.1) \\ y_k = Y_c + r_k^{ANN} \sin(\varphi_k) & (5.2) \end{cases}$$

A new circle centre was calculated with transformed coordinates as:

$$(x_c, y_c) = (u_c, v_c) + (\bar{x}, \bar{y}), \tag{6}$$

where a "best fit" circle of least squares of simulated points with the circle centre (u_c, v_c) was found from following system:

$$\begin{cases} u_c \sum_k u_k^2 + v_c \sum_k u_k v_k = \frac{1}{2}\left(\sum_k u_k^3 + \sum_k u_k v_k^2 \right) & (7.1) \\ u_c \sum_k v_k u_k + v_c \sum_k v_k^2 = \frac{1}{2}\left(\sum_k v_k^3 + \sum_k v_k u_k^2 \right) & (7.2) \end{cases}$$

Where $u_k = x_k - \bar{x}$ and $v_k = y_k - \bar{y}$ are the transformed coordinates. Then, the radius values for each point can be calculated as following:

$$\rho_k = \sqrt{(x_k - x_c)^2 + (y_k - y_c)^2} \,. \tag{8}$$

The circle centre (x_c, y_c) and radius values ρ_k are calculated in the each iteration. Then the radius variation range of the *n*-sample for each particular location is estimated by the residual $\Delta\rho = \rho_{\max} - \rho_{\min}$. Eventually, after all iterations were completed, the smallest estimated radius variation range $\Delta\rho_{\min}$ for the particular sample size *n* was defined. The maximum estimation error $\delta_{\max}$ due to the sample size *n* was calculated as $\delta_{\max} = \Delta R^{ANN} - \Delta\rho_{\min}$, where $\Delta R^{ANN} = R_{\max}^{ANN} - R_{\min}^{ANN}$ is the precise radius variation range estimated from 480 variables, which were simulated with the continuous virtual profile.

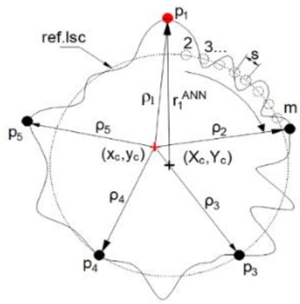

Fig. 4. The five-point sample: $p_2, p_3, ... p_n$ – the measured points; $\rho_1, \rho_2, ... \rho_5$ – the estimated radius variables; *ref.lsc* – reference least squares circle; r_1^{ANN} – a radius of the original reference circle; (X_c, Y_c) – a reference circle center based on 480 points; (x_c, y_c) – a new circle center based on 5 points**.**

5 Results and Discussion

The simulation procedure described in section 3 was applied with different sample sizes from 5 to 400 measuring points, and for 9 circle sections with nominal diameter from 40 mm to 500 mm. The final simulation results are tabulated in Table 1.

The graphical interpretation of the results (see Fig. 5a) shows that relation between the maximum estimated error $\delta_{\max}$ and the sample size *n* has nonlinear, asymptotic behavior. This behavior appears relatively predictable. However, the relation between the maximum estimated error and the diameter size for a given sample size does not follow a clear trend, when a five point-sample is used (see Fig.5b). The maximum estimated error for different diameters varies between 7.1 µm and 30.2 µm. In our tests, the maximum estimated error is up to 6.6 µm for the ninety three points sample size, and up to 2.1 µm for three hundred measuring points.

6 Conclusion

According to the simulation results, the error due to the sample size can be a significant contributor to the measurement uncertainty and thus, it must be considered in the measuring strategy for CMM.

The simulation procedure presented in this paper is a new algorithm for estimating the maximum error due to number of the measuring points. As shown with the test pieces, the diameter size is not the main factor for defining the sample strategy.

Table 1. The maximum estimated error $\delta_{\max}$ due to the sample size *n* for various diameters D_i

Sample size *n*	**5**	**15**	**30**	**60**	**93**	**150**	**200**	**300**	**400**
D_1 = 40 mm *	11.2	7.5	5.0	4.3	3.1	2.8	2.5	1.3	0.7
D_2 = 80 mm	10.2	5.4	5.0	4.1	2.5	1.9	1.6	1.1	0.5
D_3 = 100 mm	7.1	4.9	4.0	3.1	2.5	2.0	1.3	0.7	0.4
D_4 = 150 mm	21.4	11.5	9.1	7.3	6.6	6.6	4.5	2.1	0.8
D_5 = 200 mm	15.1	4.4	2.0	0.9	0.7	0.3	0.2	0.1	0.1
D_6 = 250 mm	30.2	7.8	2.6	1.9	1.1	0.7	0.7	0.4	0.0
D_7 = 300 mm	22.2	8.7	5.9	3.7	2.1	1.4	1.3	1.0	0.8
D_8 = 400 mm	21.5	8.7	4.1	1.8	1.6	1.1	0.7	0.4	0.2
D_9 = 500 mm	24.3	10.6	7.8	7.8	5.0	3.2	3.2	1.9	0.8

* $\delta_{\max}$ is given in μm

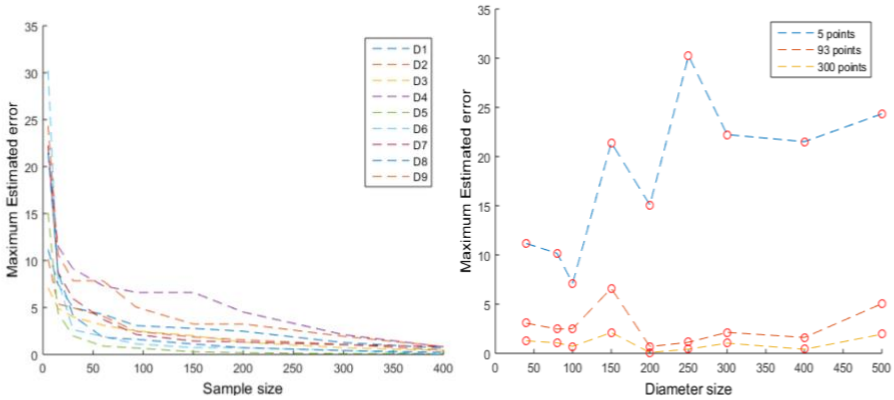

(a) The maximum estimated error vs sample size for diameters $D_1, D_2, ...D_9$

(b) The maximum estimated error vs diameter size for samples of 5, 93 and 300 points

Fig. 5. The relationship of the maximum estimated error with the sample size and the diameter size of circle profiles

The presented ANN approach can be adapted to profile forms generated by any machine operations. The approximated nondeterministic profile can be further used as the continuous function for other simulations regarding the sample strategy, alignment, filtration methods and measuring uncertainty estimation.

Reference

1. L.De Chiffre (2015) Geometrical Metrology and Machine Testing. DTU Mechanical Engineering

2. K. D. Summerhays (2002) Optimizing discrete point sample patterns and measurement data analysis on internal cylindrical surfaces with systematic form deviations. Precision Engineering 26 (1):105-121

3. Cui Changcai (2009) Research on the uncertainties from different form error evaluation methods by CMM sampling. The International Journal of Advanced Manufacturing Technology 43 (1):136-145

4. Moroni (2010) Coordinate Measuring Machine Measurement Planning. London: Springer London, London

5. Mesay T. Desta (2003) Characterization of general systematic form errors for circular features. International Journal of Machine Tools and Manufacture 43 (11):1069-1078

6. Jiang Qimi (2006) A roundness evaluation algorithm with reduced fitting uncertainty of CMM measurement data. Journal of Manufacturing Systems 25 (3):184-195

7. Cho (2001) Roundness modeling of machined parts for tolerance analysis. Precision Engineering 25 (1):35-47

8. S. Ruffa (2013) Assessing measurement uncertainty in CMM measurements: comparison of different approaches. IntJMetrol Qual Eng 4:163-168

9. Moschos Papananias A novel method based on Bayesian regularized artificial neural networks for measurement uncertainty evaluation. In: EUSPEN, Proceedings of the 16th International Conference of the European Society for Precision Engineering and Nanotechnology, Nottingham, UK, 2016. EUSPEN, pp 97-98

10. Y F Zhang (1996) A neural network approach to determinig optimal inspection sampling size for CMM. Computer Integrated Manufacturing Systems 9:p.161-169

11. Grossberg (1982) Studies of the Mind and Brain. Reidel Press, Drodrecht, Holland

12. Wang (2007) Applied computational intelligence in intelligent manufacturing systems, vol vol. 2. International series on natural and artificial intelligence, 2nd ed. edn. Advanced Knowledge International, Adelaide, S.Aust

13. Jones (1987) Back-propagation: a generalized delta learning rule. Byte 12 (11):155-162

14. Mark Hudson Beale (2017) Neural Network Toolbox, User guide

15. Marquardt (1963) An Algorithm for Least-Squares Estimation of Nonlinear Parameters. SIAM Journal on Applied Mathematics 11:431–441